Indian J. Vet. Surg. 46(2): 84-87 December 2025

ijvs

Computed Tomography of thyroid gland in dogs

Narendra Singh[1†], P. Bishnoi[2], Sakar Palecha[3], A.K. Bishnoi[3], Shivangi Diwedi[1], Komal Galgat[1], Ruchi Patwa[1] and Ankita Kumari[1]

Rajasthan University of Veterinary and Animal Sciences, Bikaner-334 001 (Rajasthan)

[1]PhD Scholar, [2]Professor and Head,[3] Assistant Professor, Department of Veterinary Surgery and Radiology, College of Veterinary and Animal Science, Bikaner

DOI: 10.5958/0973-9726.2025.00024.3 *Received: February, 2024*

The present study evaluated the computed tomography (CT) characteristics of the thyroid gland in dogs by assessing its appearance and attenuation values in healthy and hypothyroid animals. A total of 12 healthy dogs and 8 dogs diagnosed with hypothyroidism were included. The mean age and body weight were 4.25 yr and 16.10 kg in healthy dogs, and 7.65 yr and 34.13 kg in hypothyroid dogs, respectively. On transverse and multi-planar reconstructed images, the thyroid gland was assessed for its location relative to the trachea, lobar shape, and lowest, highest, and mean attenuation (HU) values. Dogs with hypothyroidism had significantly lower pre-contrast mean attenuation values (64.48±2.49 HU) compared to healthy dogs (79.93±2.32 HU). Similarly, post-contrast attenuation values were significantly reduced in hypothyroid dogs (101.29±4.47 HU) compared to those with normal thyroid function (122.84±4.86 HU). In conclusion, hypothyroidism is associated with a significant decrease in both pre- and post-contrast CT attenuation values of the thyroid gland. The CT features identified in healthy dogs provide reliable criteria for locating and evaluating the thyroid gland in cervical CT imaging.

***Key words**: Computed Tomography, Diagnostic Imaging; Dog, Thyroid gland*

Modern diagnostic procedures, particularly advanced imaging techniques, are routinely employed to achieve accurate diagnosis of various clinical conditions. In thyroid disorders, diagnostic imaging not only facilitates identification of the underlying disease but also plays a crucial role in guiding treatment and assessing prognosis. The rapid development of imaging modalities has greatly improved diagnostic precision and accessibility. Among these modalities, ultrasonography, computed tomography (CT), magnetic resonance imaging, and scintigraphy are commonly used to evaluate thyroid diseases, each offering distinct advantages and limitations (Taeymans *et al*., 2007; Singh *et al*., 2021).

Computed tomography (CT) is considered one of the most effective imaging tools for evaluating the thyroid gland owing to its superior spatial resolution and ability to generate reproducible and accurate measurements of thyroid size. CT provides cross-sectional images that allow detailed visualization of internal cervical structures, overcoming the limitations of conventional radiography caused by tissue superimposition. Additionally, CT is particularly useful for detecting thyroid tissue because normal thyroid parenchyma tends to be hyper attenuating due to its intrinsic iodine content. In contrast, diseased thyroid tissue in humans often appears isoattenuating or hypoattenuating relative to adjacent musculature in pre-contrast CT images (Hermans *et al*., 1997; Imanishi *et al*., 2000). CT also offers the added advantage of screening for pulmonary metastatic disease during the same examination.

Reported CT attenuation ranges for the normal thyroid gland in pre- and post-contrast studies are approximately 87–137 HU and 125–230 HU, respectively (Daminet and Ferguson, 2003; Taeymans *et al*., 2008; Wisner and Zwingenberger, 2015; Maldjian and Chen, 2016). Considering the extensive information available from human studies and the limited but growing research in canine thyroid imaging, the present study was undertaken to evaluate the computed tomographic characteristics of the thyroid gland in healthy dogs as well as dogs affected with hypothyroidism.

Materials and Methods

This prospective analytical study was conducted following approval from the Institutional Animal Ethics Committee (IAEC), Rajasthan University of Veterinary and Animal Sciences, Bikaner (Approval No. CVAS/IAEC/2022-23/31 dated 01.11.2022).

Twenty dogs presented to the Veterinary Clinical Complex, College of Veterinary and Animal Science, Bikaner, between November 2022 and December 2023 were enrolled. Of these, 12 dogs were classified as healthy and eight were diagnosed with hypothyroidism based on serum thyroid hormone assay (T3 and T4 concentrations).

The mean age of healthy dogs was 4.25 yr (range: 12 m - 10 yr), and the mean body weight was 16.10 kg (range: 10–25 kg). Breeds represented included mixed breed (n=7), Labrador Retriever (n=3), Doberman Pinscher (n=1), and Golden Retriever (n=1). All dogs were clinically healthy, with normal CBC and biochemical profiles, and presented with complaints

†Corresponding author; E-mail: narendravet@gmail.com

unrelated to thyroid disease. These dogs underwent CT examination for various reasons including orthopedic conditions (n=6), lameness (n=2), and neurologic signs associated with intervertebral disc disease (n=4). Thyroid gland evaluation was included during these CT studies.

Dogs clinically diagnosed with hypothyroidism included Labrador Retriever (n=5), German Shepherd (n=2), and Pug (n=1). The group comprised three males and five females. The mean age was 7.65 yr (range: 2 years 7 m -12 yr), and the mean body weight was 34.13 kg (range: 12–47 kg). All were subjected to CT examination as part of the study.

All dogs underwent CT scanning under general anaesthesia. Xylazine HCl (1 mg/kg, body weight IM) was administered as premedication, followed by ketamine HCl (5 mg/kg, IM) for induction. Endotracheal intubation was performed using an appropriately sized tube to maintain airway patency throughout the procedure.

CT examinations were performed using a 16-slice CT scanner (Supria, Hitachi Ltd.). Dogs were positioned in dorsal recumbency in a head-first orientation (Fig. 1), with forelimbs retracted caudally to prevent superimposition over the cervical region. The neck was positioned to ensure the thyroid gland was perpendicular to the X-axis of the gantry. Scanning was performed using the following parameters: slice thickness 0.625–1.25 mm, 120 kV, 50–90 mA, and a field of view adjusted according to patient size. Axial contiguous images were obtained from the caudal aspect of the cricoid cartilage to approximately 8 cm caudally.

Post-contrast CT was performed following the intravenous administration of non-ionic, iodinated contrast agent iohexol (Contrapaque-350; 350 mg/mL; J.B. Chemicals and Pharmaceuticals Ltd., Mumbai) @ 600 mg/kg body weight through the cephalic vein. Images were acquired approximately 30 s after injection (Amoros *et al.*, 2021). Dogs without contrast-enhanced scans were excluded from the study. Identical scan settings were used for both pre- and post-contrast series.

Volume data were reconstructed using bone and soft-tissue algorithms in isotropic transverse, sagittal, and dorsal planes. The trachea and cervical spine served as midline anatomic reference points. Window width and level were standardized: soft tissue: WW = 400 HU, WL = –40 HU; bone: WW = 2700 HU, WL = 350 HU. A subjective visual assessment of thyroid lobe homogeneity was performed in both pre- and post-contrast images. The lowest, highest, and mean attenuation values (HU), location relative to the trachea, and lobe shape were recorded using transverse and multiplanar reconstructed images (Fig. 1).

Regions of interest (ROIs) were manually drawn around each thyroid lobe on every transverse slice that

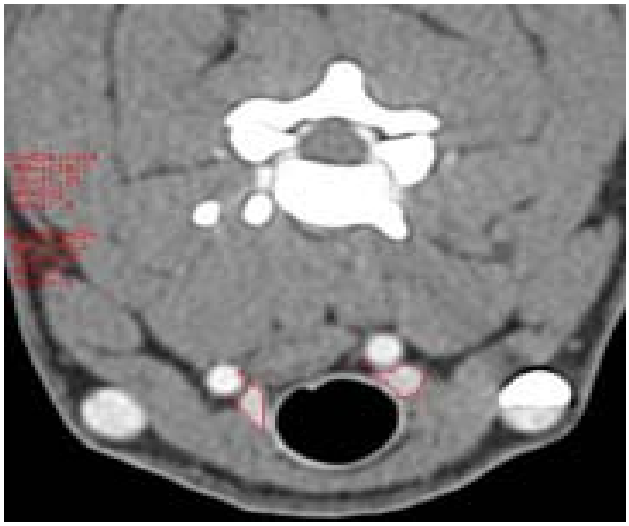

(A)

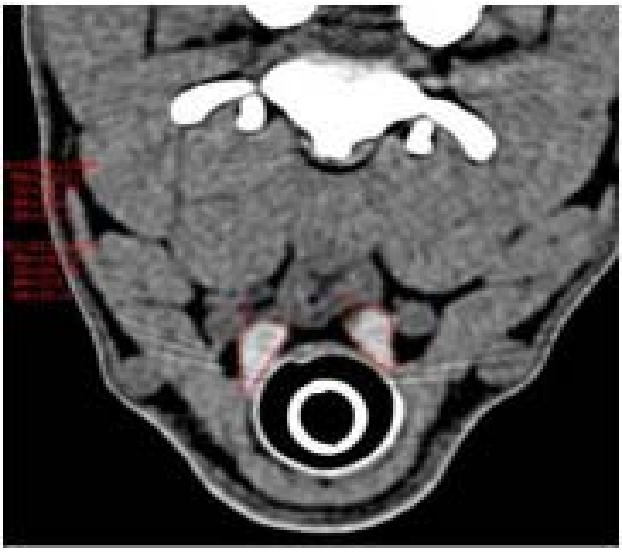

(B)

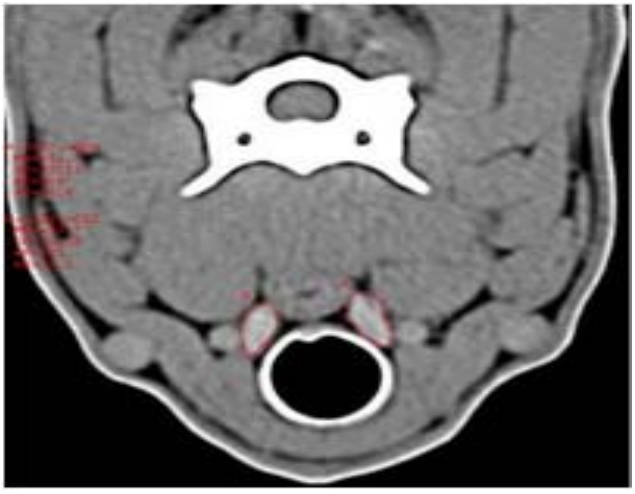

(C)

Fig.1: The CT images (A, B and C) in transverse plane demonstrating manually drawn Region of Interest (ROI) around each transverse section of thyroid lobe for calculation of attenuation value of ROI section in pre- and post– contrast series in dogs.

included thyroid tissue in both pre- and post-contrast series. The CT workstation automatically calculated the mean HU, standard deviation, and ROI surface area. For each dog, the overall mean attenuation value was determined by averaging the mean HU of all transverse sections from both lobes. Lowest, highest, and mean attenuation values were documented.

Mean attenuation values and thyroid volume were analyzed using analysis of variance (ANOVA) followed by a critical difference test for pairwise comparison of means (Snedecor and Cochran, 1967). Statistical significance was set at $P < 0.05$.

Results and Discussion

Subjective visual assessment of the thyroid lobes in both pre- and post-contrast CT images revealed that all lobes in healthy dogs and nearly all in hypothyroid dogs were homogeneous, consistent with the findings of Amoros *et al.* (2021). Only one dog exhibited heterogeneous attenuation on pre-contrast imaging, similar to observations by Weissman *et al.* (1998).

The shape of the thyroid lobes on transverse CT images in healthy dogs was predominantly ovoid (54.17%), followed by oval (33.33%) and triangular (12.50%) **(Table 1).** In hypothyroid dogs, lobes were primarily ovoid (62.50%), with oval (25%) and polygonal (12.50%) shapes (Table 2). These patterns are in agreement with earlier descriptions in dogs and other species (Drost *et al*., 2004; Pankowski *et al*., 2021). On dorsal-plane reconstructions, healthy dogs showed elongated ovoid (66.67%) and elliptical (33.33%) shapes, whereas hypothyroid dogs predominantly had elliptical lobes (87.50%). These configurations are consistent with previously published CT descriptions in domestic animals.

The thyroid lobes were most commonly located dorsolateral to the trachea in both study groups (Table 3), similar to the findings of Taeymans *et al*. (2008), although no lateral or ventrolateral positions were recorded in the present study. Reported anatomical variations in cats and goats (Pankowski *et al*., 2021) were not observed. The right thyroid lobe was consistently positioned more cranially than the left, with mean cranial locations of 1.41 and 2 tracheal rings in healthy dogs, closely matching earlier studies (Taeymans *et al*., 2008). Caudal extent of the lobes also corresponded with the expected range (4–8 tracheal rings), providing reliable anatomical landmarks for thyroid identification and assessment.

In this study, the thyroid glands were readily identified on both pre- and post-contrast images. Significant differences in pre-contrast and post-contrast mean attenuation values were noted between healthy and hypothyroid dogs. Hypothyroid dogs demonstrated significantly lower mean attenuation in both series (pre-contrast: 64.48±2.49 HU; post-contrast: 101.29±4.47 HU) compared with healthy dogs (pre-contrast: 79.93±2.32 HU; post-contrast: 122.84±4.86 HU) (Table 4). These findings align with earlier reports indicating that normal thyroid tissue appears hyperattenuating owing to its intrinsic iodine content (Taeymans *et al*., 2008; Silverman *et al*., 1984). Lower attenuation in diseased thyroid tissue has been attributed to reduced follicular iodine content, cellular changes, or interstitial alterations. Breed-related differences in attenuation, as reported by Amoros *et al*. (2021), may also influence results but were not assessed here.

Table 1: The shape of the lobes on transverse and dorsal plane in healthy dogs.

Sl. No.	Plane of CT	Shape	No. of lobes		
			Left lobe	Right lobe	Total
1.	transverse	ovoid	06	07	13
2.		oval	04	04	08
3.		triangular	02	01	03
4.	dorsal plane	elongated ovoid	08	08	16
5.		elliptical	04	04	08

Table 2: The shape of the lobes on transverse and dorsal plane in dogs with hypothyroidism.

Sl. No.	Plane of CT	Shape	No. of lobes		
			Left lobe	Right lobe	Total
1.	transverse	ovoid	05	05	10
2.		oval	02	02	04
3.		polygonal	01	01	02
4.	dorsal plane	elliptical	07	07	14
5.		ovoid	01	01	02

Table 3: Location of thyroid gland (in relation to tracheal rings) in healthy dogs and dogs with hypothyroidism.

Position	Healthy dogs		Dogs with hypothyroidism	
	Right lobe	Left lobe	Right lobe	Left lobe
Cranial location	1.41 (1-2)	2 (1-3)	1.38 (1-2)	2 (1-3)
Caudal location	5.5 (4-7)	6.17 (4-8)	5.38 (4-7)	6.13 (5-7)

Post-contrast attenuation values in this study were lower than previously reported in dogs and cats (Drost *et al*., 2004). As contrast enhancement primarily reflects vascular perfusion, minor variations in natural iodine

Table 4: Attenuation value (pre- and post-contrast) of thyroid gland in healthy dogs and dogs with hypothyroidism.

Group	Pre-contrast (Mean±SE and range)			Post-contrast (Mean±SE and range)		
	Right	Left	Overall	Right	Left	Overall
Normal	77.93^{b}±3.19	81.95^{b}±3.40	79.93^{b}±2.32	120.71^{d}±6.92	124.98^{d}±6.95	122.84$^{d±}$4.86
	(51.8-103.3)	(51.4-111)		(57.2-187.3)	(62.3-192.7)	
Hypo	63.54^{a}±3.23	65.43^{a}±3.88	64.48^{a}±2.49	100^{c}±6.46	102.6^{c}±6.38	101.29^{c}±4.47
	(40.3-83.3)	(41.5-88)		(65.5-155.2)	(66.9-140)	

content have limited effect on post-contrast attenuation (Mettler and Guiberteau, 2019). No significant differences between right and left thyroid lobes were observed in either healthy or hypothyroid dogs.

The study population for the healthy group consisted of dogs presented for orthopedic or neurologic conditions rather than clinically normal dogs. However, all had normal haematological profiles and thyroid hormone assays, consistent with Amoros *et al*. (2021). Hypothyroidism was diagnosed based on clinical signs and thyroid hormone assays, though limitations such as assay variability and small sample size should be considered (Dixon and Mooney, 1999; Daminet and Ferguson, 2003).

Thyroid hormone profiles confirmed normal T3, T4, and TSH levels in healthy dogs, while hypothyroid dogs showed markedly reduced T3 and T4 concentrations (Table 5). Despite the limited sample size, the study demonstrates that CT imaging reliably depicts thyroid morphology, location, and attenuation characteristics in both healthy and hypothyroid dogs.

CT is a valuable imaging modality for evaluating the canine thyroid gland. Normal thyroid tissue is readily identifiable on pre-contrast images due to its higher attenuation relative to surrounding tissues and shows strong enhancement on post-contrast studies. Dogs with hypothyroidism exhibit significantly reduced attenuation values in both pre- and post-contrast scans. Overall, CT provides reliable anatomical and attenuation-based criteria for identifying and assessing the thyroid gland in dogs.

References

Amoros, O., Espada, Y., Vila, A., Jimenez, A. and Novellas, R. 2021. Pre contrast CT attenuation of the thyroid gland is lower in brachycephalic dogs versus non brachycephalic dogs. Vet. Radiol. Ultrasound **62**: 54-60.

Daminet, S. and Ferguson, D. 2003. Influence of drugs on thyroid function in dogs. J. Vet. Intern. Med. **17**: 463-472.

Dixon, R.M. and Mooney, C.T. 1999.Evaluation of serum free thyroxine and thyrotropin concentrations in the diagnosis of canine hypothyroidism. J. Small Anim. Pract. **40**: 72-78.

Drost, W.T., Mattoon, J.S., Samii, V.F., Weisbrode, S.E. and Hoshaw Woodard, S.L. 2004. Computed tomographic densitometry of normal feline thyroid glands. Vet. Radiol. Ultrasound **45**: 112-116.

Hermans, R., Bouillon, R., Laga, K., Delaere, P.R., Foer, B.D., Marchal, G. and Baert, A.L. 1997. Estimation of thyroid gland volume by spiral computed tomography. Eur. Radiol. **7**: 214–216.

Imanishi, Y., Ehara, N., Shinagawa, T., Tsujino, D., Endoh, I., Baba, K. and Nosaka, S. 2000. Correlation of CT values, iodine concentration, and histological changes in the thyroid. J. Comput. Assist. Tomogr. **24**: 322-326.

Maldjian, P. and Chen, T. 2016. Is visual assessment of thyroid attenuation on unenhanced CT of the chest useful for detecting hypothyroidism? Clin. Radiol. **71**: 1199.e9-1199.e14.

MettlerJr, F.A. and Guiberteau, M.J. 2019. Essentials of nuclear medicine imaging: expert consult-online and print. Philadelphia, PA: Elsevier Health Sciences. p 85.

Pankowski, F., Bartyzel, B.J., Pasko, S., Moroz, A., Mickiewicz, M., Szalus-Jordanow, O. and Bonecka, J. 2021. CT appearance and measurements of the normal thyroid gland in goats. BMC Vet. Res.**17**: 1-8.

Singh, S., Palecha, S., Bishnoi, P. and Gahlot, T.K. 2021. Evaluation of degenerative changes of elbow and coxo-femoral jointsin dogs using computed tomography. Indian J. Vet. Surg. **42**: 84-90.

Silverman, P.M., Newman, G.E., Korobkin, M., Workman, J.B., Moore, A.V. and Coleman, R.E. 1984. Computed tomography in the evaluation of thyroid disease. Am. J. Roentgenol. **142**: 897-902.

Snedecor, G.W. and Cochran, W.G. 1967. Statistical Methods, 6th edn. Ames, Iowa: The Iowa State University Press, USA.

Taeymans, O., Peremans, K. and Saunders, J.H. 2007. Thyroid imaging in the dog: current status and future directions. J. Vet. Inter. Med. **21**: 673-684.

Taeymans, O., Schwarz, T., Duchateau, L., Barberet, V., Gielen, I., Haskins, M., Van Bree, H. and Saunders, J.H. 2008. Computed tomographic features of the normal canine thyroid gland. Vet. Radiol. Ultrasound **49**: 13-19.

Weissman, J.L., Curtin, H.D. and Johnson, J.T. 1998. Thyroid gland after total laryngectomy: CT appearance. Radiol. **207**: 405–409.

Wisner, E. and Zwingenberger, A. 2015.Atlas of Small Animal CT and MRI. Ames: John Wiley & Sons, p 141.